Nanoscale

Accepted Manuscript

This article can be cited before page numbers have been issued, to do this please use: Y. Li, W. Li, K. He, P. Li, Y. Huang, Z. Nie and S. Yao, *Nanoscale*, 2016, DOI: 10.1039/C6NR01072E.

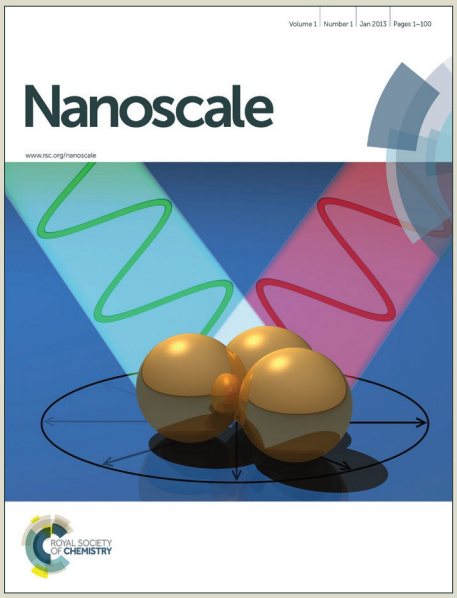

ROYAL SOCIETY OF CHEMISTRY

www.rsc.org/nanoscale

View Article Online
DOI: 10.1039/C6NR01072E

Nanoscale

Full Paper

A biomimetic colorimetric logic gate system based on multi-functional peptide-mediated gold nanoparticles assembly

Received 00th January 20xx,
Accepted 00th January 20xx

DOI: 10.1039/x0xx00000x

www.rsc.org/

Yong Li, Wang Li, Kai-Yu He, Pei Li, Yan Huang, Zhou Nie,* and Shou-Zhuo Yao

In natural biological system, proteins exploit various functional peptide motifs to exert target response and activity switch, providing functional and logic basis for complex cellular activities. Building biomimetic peptide-based bio-logic systems is highly intriguing but remains relatively unexplored due to limited logic recognition elements and complex signal outputs. In this proof-of-principle work, we attempted to address these problems by utilizing multi-functional peptide probes and the peptide-mediated nanoparticle assembly system. Here, the rational-designed peptide probes function as dual-target responsive element specifically responsive to metal ion and enzyme as well as the mediator regulating the assembly of gold nanoparticles (AuNPs). Taking advantage of Zn^{2+} ion and chymotrypsin as the model inputs of metal ion and enzyme, respectively, we constructed the peptide logic system computed by the multi-functional peptide probes and outputted by readable colour change of AuNPs. In this way, reprensative binary basic logic gates (AND, OR, INHIBIT, NAND, IMPLICATION) have been achieved through delicately coding the peptide sequence, demonstrating the verstility of our logic system. Additionally, we demonstrated that the three-input combinational logic gate (INHIBIT-OR) could also be successfully integrated and applied as a multi-tasking biosensor for colorimetric detection of dual targets. This nanoparticles-based peptide logic system presents a valid strategy to illustrate pepitde information processing and provides a practical platform for excuting peptide computing or peptide-related multiplexing sensing, implying that the controllable nanomaterials assembly is a promising and potent methodology for the advance of biomimitic bio-logic computation.

Introduction

Biomolecular logic gate is the fundamental unit of biocomputer, which mimics electronic computer to excute Boolean logic functions at molecular level through biological reactions.[1] During this programmed process, it performs operation of sensing inputs, processing the input information for decision-making, and executing the readable outputs. In this way, it can greatly enhance our ability to understand complex biological events, including gene expression regulation, enzymatic activity regulation and signal transduction networks[2]. Also, rational design and engineering of biomolecular logic gate holds potential applications in logic sensing, intelligent diagnostics, and robotic diagnosis.[3, 10] To date, several biomolecules, including DNA/RNA[4], enzymes[5] and even whole cells[6] have been employed as building blocks for logic gate construction. In particular, DNA molecules (*e.g.*, aptamers and DNAzymes) has been exploited in various logic devices, with remarkable progress from basic logic gates (AND, OR, XOR, NAND, NOR, INHIBIT, *etc.*) to complex logic applications, such as simulating human memory[7], computational mathematics[8], game program addition[9] and disease diagnosis or therapy[10]. Another key biomolecule, peptide, on the other hand, has rarely been applied to building practical logic gate systems. The only example of such peptide application to our knowledge is Ashkenasy's work, which was engaged in creating peptide-based catalytic networks for Boolean logic operations.[11] Although the antibody-based peptide computation model has been theoretically proposed, it remains unrealized in practice[12]. Hence, the establishment of a rational peptide-based logic system, where the coded peptide could logically respond to inputs and then yield intuitive output signals, is still highly challenging.

Since a peptide consists of 20 standard amino acids and other rare amino acids, it possesses much greater sequence diversity than nucleic acid. Consequently, it supplies tremendous structural possibilities for fulfilling various complicated biological activities, such as biorecognition and interaction during cellular differentiation[13], signal transmission[14], immune defense[15], cell apoptosis[16, 20] and so on[17]. One typical example is metal ion-recognition peptide segments, where the representative one is the Ca^{2+}-binding motif in calmodulin (CAM), which specifically chelates Ca^{2+} to regulate the Ca^{2+}/CAM-dependent kinase signal transduction.[19] Other examples are specific substrate peptide segments that can be recognized and cleaved by proteases. During the cell

State Key Laboratory of Chemo/Biosensing and Chemometrics, College of Chemistry and Chemical Engineering, Hunan University, Changsha, 410082, P. R. China. E-mail: niezhou.hnu@gmail.com; Fax: +86-731-88821848; Tel: +86-731-88821626;

Electronic Supplementary Information (ESI) available: additional figures (Table S1-3, Figure S1-S6). See DOI: 10.1039/x0xx00000x

View Article Online
DOI: 10.1039/C6NR01072E

apoptosis process, activated caspase 3/7 recognize and cleave the specific peptide sequence (DEVD) of the substrate death.[20] Thus, peptides regulation of natural biofunctional processes indicate that peptides are switchable via recognition or interaction with biomolecules. It follows, then, that mimicking these biological events presents a series of promising building blocks for developing a peptide logic system *in vitro*.

One of the obvious obstacles to creating such a logic system is how to convert the inputs received through peptide recognition to easily readable output signals after logic manipulation by peptide switches. Traditional methods use reversed-phase high performance liquid chromatography (RP-HPLC) and mass spectrometry (MS) to present output signals for peptide logic gates. However, these methods are discontinuous, heterogenous, complex, and time-consuming. Fortunatley, the rapid growth of nanotechnology in recent years provides new opportunities to overcome these obstacles. As a potent biomaterial with multiple functional side groups, peptides have been variously used as template, ligand, protectant and surface decorator for controlling growth and regulating self-assembly of various inorganic nanomaterials.[21] The unique plasmonic properties of gold nanoparticles (AuNPs) have attracted particular attention for their use in peptide-mediated AuNP generation and assembly. Peptides have been used to modify the surface of AuNPs to control their size, shape, and morphology. Mandal and co-workers prepared peptide-functionalized AuNPs and demonstrated that various heavy metal ions (Pb^{2+}, Cd^{2+}, Cu^{2+} and Zn^{2+}) could impel these decorated AuNPs to self-assemble into two- or three-dimensional nanostructures in an aqueous solution.[22] Furthermore, through rational design of peptide sequences, the peptide could recognize the target and mediate the dispersibility of AuNPs. Modulation of the dispersibility of AuNPs, accompanied with the plasmonic property, changes the solution colour in an on-off/off-on manner[23-27]. In addition, AuNPs-based colorimetric signal output is facile and convenient for logic gate construction[28]. Hence, target-responsive peptide-mediated AuNPs assembly could directly convert peptide recognition to AuNPs-dependent optical signal change, which shows great potential for developing a simple and homogenous signal outputs for a peptide-based logic system.

Herein, we develop a novel and versatile peptide logic system that rationally integrates a peptide-dependent logic computing center and an AuNPs-based colorimetric signal output system. To mimic natural proteins responsive to specific metal ion or enzyme, a set of multi-functional peptide probes were rationally designed to function as dual-target responsive element specifically responsive to metal ion (zinc ion, one of the most important co-factors in the regulation of in physiological, metabolic pathways, and apoptosis) and protease (chymotrypsin, Chy, normally secreted by pancreatic acinar cells for food digestion) as well as the mediator regulating the assembly of gold nanoparticles (AuNPs). Two functional peptide motifs, the zinc ion-chelating peptide and the protease substrate peptide, were used as the fundamental input-recognition components that are specifically responsive to Zn^{2+} and Chy, respectively. Integrating these input recognition components into the peptide probe and carefully balancing the positively net charge of peptide can regulate the aggregation of the negatively charged AuNPs, leading to a target-responsive color switch of AuNPs solution. Based on this mechanism, basic binary logic gates (e.g., OR, AND, NAND, IMPLICATION, and INHIBIT) were developed using peptide-mediated AuNP assembly system. These basic binary logic gates can then be cascaded down into combinational gates, like INHIBIT-OR, which was implicated in multi-tasking biosensing of dual targets. Hence, this nanoparticles-dependent biomimetic peptide logic system might pave the way for developing complicated peptide-based Boolean computing.

proteins/enzymes, which leads to the functional damage of these proteins/enzymes and the subsequent programmed cell

Result and Discussion

Description of the peptide logic system

To develop this peptide logic gate system, 13 nm citrate-capped AuNPs were chosen as the output signal indicator. The dispersed AuNPs can be identified by the red colour because of the localized surface plasmon resonance (LPSR). Further, the colloidal stability of the AuNPs is sensitive to variations on their negative surface charge. Postively charged peptide with cysteine residue can readily anchor onto the surface of AuNPs via thiol-gold interaction, which would neutralize the surface negative charges and impel AuNPs to aggregation. In an aggregated state, interparticle plasmon coupling would induce a significant colour change from red to blue/purple in solution (Scheme 1a). Accordingly, all the peptide probes were artificially designed and endowed with two AuNPs-regulating parts: the binding group, cysteine (C) residue, to anchor the peptide onto the surface of the AuNPs, and the charged group, arginine (R) residue, to vary the surface charge of AuNPs. These two parts co-operate and contribute to the aggregation-induced colour change (AICC) of AuNPs. Thus, by rationally coding proper recognition components for target-response with two AuNPs-regulating parts into the peptide sequence, the peptide probes can control the readable colorimetric signal of AuNPs in a switchable manner.

Peptide motif CCPGC has a high affinity for Zn^{2+} because of the strong chelation among all three cysteine residues and Zn^{2+}[29]. In view of that, we coded the Zn^{2+}-chelating peptide (CCPGC) with the charged group (Arg) to form the Zn^{2+}-responsive peptide probe, hoping the peptide would recognize the inputted Zn^{2+} and produce a Zn^{2+}-responsive colorimetric switch. As depicted in Scheme 1b, the peptide probe alone is responsible for the aggregation and corresponding red-to-blue colour change of AuNPs. But when Zn^{2+} was inputted (Mode a), CCPGC first chelates Zn^{2+} to form CCPGC-Zn^{2+} complex, thus it blocks the binding of peptide with AuNPs via three cycstine residues in CCPGC motif and

View Article Online
DOI: 10.1039/C6NR01072E

prevents the peptide-mediated AICC of AuNPs, causing AuNPs solution remaining red. This Zn^{2+}-induced AICC of AuNPs can serve as a fundamental YES gate using Zn^{2+} as the input. Additionally, a protease-responsive YES gate can be fabricated by integrating the substrate motif of protease into a peptide probe. Chymotrypsin (Chy) was chosen as a model protease, which specifically cleaves peptide amide bonds where the carboxyl side of the amide bond is a large hydrophobic amino acid (tyrosine, tryptophan, and phenylalanine).[30] Its substrate residue, tyrosine (Y), is inserted into the peptide probe and located between two regulating parts, which will be recognized by chymotrypsin (Chy). As depicted in Scheme 1b, when Chy is added (Mode b), the peptide probe is hydrolyzed by Chy, which splits it into two short fragments. As a result, positively charged group is released from the binding group, and the neutral segment with the binding group loses its ability to induce AICC of AuNPs, thus constituting a Chy-responsive colorimetric switch.

In this way, the Zn^{2+}-chelating sequence and Chy hydrolysis substrate were coded with the binding and charged groups, respectively, to create the logic input recognition probes. Two logic manipulation modes—Zn^{2+} blocking and Chy splitting—were established to produce two independent input-responsive switches (Scheme 1b). Thus, by defining the multi-functional peptide as a computing centre, Zn^{2+} and Chy as the input elements, and colour change of AuNPs solution as the output signal, we created a versatile peptide-computed logic system, as demonstrated in Scheme 1c.

Verification of the peptide-mediated AICC of AuNPs

Prior to logic gate construction, we investigated the binding capacity and charge property of peptides in relation to AICC of AuNPs. Three designed peptides with different net charges were considered. The cationic peptide, P-1 (CAAR, 5 μM), quickly induced an AICC of AuNPs from red to blue (Fig. 1a), as well as an apparent redshift of the absorption peak from 520 nm to 610 nm, and aggregation of dispersed AuNPs to larger particles (Fig. 1c, d). It is worthy to note that the peptide-induced aggregation is completed in just 1 min (Fig. S1), indicating the quick response of this colorimetric switch. Oppositely, the anionic peptide, P-8 (DDDYCCPGC, 5 μM), and neutral peptide, P-9 (CCPGC, 5 μM), did not induce any apparent changes in the solution colour, the UV-vis absorption spectrum, or the particle size of AuNPs, all of which revealed the well-dispersed state of AuNPs (Fig. 1). Meanwhile, after the addition of P-1, the negative net charge of AuNPs decreased sharply to neutral or slight positive (Zeta potential from -24 mV to +4 mV), while P-8 and P-9 retained a negative net charge in AuNPs, which resulted in electrostatic repulsion strong enough to keep them well-stabilized (Fig. 1b and Fig. S2). These results confirmed that the peptide with both the binding group and the positively charged group possesses high binding affinity and electrostatic interaction with AuNPs, leading to quick aggregation as well as an obvious colour change of LSPR shift from red to blue/purple.

Fabrication of the Zn^{2+}/Chy-responsive colorimetric switch

Based on the peptide-mediated AICC of AuNPs, a Zn^{2+}-responsive peptide probe, P-2 (CCPGCAR), was designed by integrating the positively charged group R with the CCPGC motif for both the AuNP-binding and Zn^{2+} chelating. As shown in Fig. 2a, the P-2-mediated AICC of AuNPs would be completely suppressed by Zn^{2+}, meaning the solution colour of AuNPs would be tunable according to the presence or absence of Zn^{2+}. This constitutes a Zn^{2+}-responsive colorimetric switch and may be defined as a basic YES logic gate. The addition of Zn^{2+} or not was defined as inputting state "1" or "0", respectively. Meanwhile, because the dispersion state of AuNPs could be judged by the solution colour and quantified through the solution absorption ratio of A_{520}/A_{610}, we set the red solution as a true output of "1", while a false output of "0" represents the blue/purple solution, and the ratio value for A_{520}/A_{610} was set at 2.0 as the threshold value to further define the logic output. Under the optimized condition (Fig. S3), blue AuNPs were observed with the input of "0", and two considerable peaks detected at about 520 nm and 610 nm (black line in Fig. 1c) with a ratio of A_{520}/A_{610} at 1.08 (blue column in Fig. 2e), revealing the output of "0"; yet when Zn^{2+} was inputted in the state of "1", only one absorption peak at 520 nm (Fig. 2c, red line) was observed, and the red solution generated a ratio of A_{520}/A_{610} of 3.4, representing the output of "1", which actually implemented the switch function of a Zn^{2+}-triggered YES logic gate (Fig. 2g). Similarly, a Chy-responsive colorimetric switch was also created and could be translated to a YES logic gate. Fig. 2b shows that the Chy-responsive peptide probe P-3 (CAYRA, containing a Chy cutting site Y in the middle) can also induce an AICC of AuNPs. As Chy was inputted under the optimized condition (Fig. S4), the AuNPs solution remained red (Fig. 2h), in accordance with the theoretical prediction that Chy-catalysed peptide cleavage separates two regulatory parts and retains the dispersion of AuNPs. Herein, Chy was taken as logic input element and AICC of AuNPs as a logic output. The input states of "0" and "1" yielded output signals of "0" and "1", respectively (Fig. 2h), along with the ratio of A_{520}/A_{610} of the blue and red solutions to be 0.74 and 4.48 (Fig. 2d), respectively, which represents a Chy-inputted YES logic gate.

Construction of the basic binary logic gates

As noted from the two YES gates, two recognition modes, Zn^{2+} chelating and Chy hydrolysis, respectively, were exploited to regulate the AICC of AuNPs. We then integrated these two recognition elements into one peptide probe to implement basic binary logic gates of dual inputs. As shown in Fig. 3a, an OR logic gate was designed first using Zn^{2+} and Chy as inputs. The OR gate peptide probe (P-4: ARYCCPGC) composed of ARY (charged group with Chy cutting site) and CCPGC (binding group for either AuNPs or Zn^{2+}). In the input state of "0/0", P-4 induced AuNPs aggregation and turned the solution colour from red to purple. When Chy existed in the state "1/0", it cleaved P-4 into two fragments (ARY and

View Article Online
DOI: 10.1039/C6NR01072E

CCPGC), and without the positively charged part (ARY), the binding part (CCPGC) alone cannot induce AICC of AuNPs (Output = 1). When Zn^{2+} was inputted in the state "0/1", similar to its action in the YES gate of Zn^{2+}, Zn^{2+} firmly chelated the three sulfydryl of CCPGC to become an ARYCCPGC-Zn^{2+} complex that inhibited the binding interaction between AuNPs and C, maintaining AuNPs in well-dispersed state (Output = 1). When Chy and Zn^{2+} coexisted in the input state of "1/1", both the cleavage of Chy and the chelating of Zn^{2+} by CCPGC motif cause the charged group dropped out from the peptide and the binding group was occupied by Zn^{2+}, which also kept the AuNPs well-dispersed (Output = 1). Accordingly, the solution colour of the four input states ("0/0", "1/0", "0/1", "1/1") were blue, red, red and red, respectively, and the related values of A_{520}/A_{610} were 1.183, 5.42, 3.425 and 5.42 (Fig. 3b, c, d), corresponding to the output "0", "1", "1" and "1" (Fig. 3d), respectively, which satisfied the binary OR logic gate.

In addition, an AND logic gate was achieved based on a modified strategy through designing a new computing peptide P-5 (ACYRCCPGC). This AND gate peptide consists of three parts: an AuNPs binding group (AC), a positively charged group with Chy cleavage site (YR), and a Zn^{2+}/AuNPs dual-binding group (CCPGC). The input states "0/0", "1/0" and "0/1" all led to AICC and displayed the output of "0" with the A_{520}/A_{610} ratio of 0.82, 1.13 and 1.65, respectively (Fig. S5b). This results from that because of this AND gate peptide containing two AuNPs-binding groups, either the Chy cleavage ("1/0") or the Zn^{2+} binding by CCPGC ("0/1") only cause the release or blocking of one of AuNP-binding group, but the another AuNPs-binding group still conjugated with the charged group (R), retaining its ability to induce AICC of AuNPs (Output = 0). In cases when Chy and Zn^{2+} co-existed in the buffer, Chy cleaved P-5 to ACY and RCCPGC, and the Zn^{2+} bound to RCCPGC. Thus two AuNPs-binding groups are separated or blocked, inactive the peptide probe to induce AICC of AuNPs, resulting in a true output "1" and a red solution colour (A_{520}/A_{610} = 5.32, Fig. S5b, c). Hence, only in the state of "1/1" could the true output of "1" be obtained, which confirmed the proper execution of an AND logic gate.

As noted above, all the constructed logic gates have a false output for the ground state ("0/0"). Nevertheless, some logic gates, such as NOR, NAND, XNOR and IMPLICATION, require a true output value of "1" in the initial ground state. Taking the IMPLICATION gate as an example, a zwitterionic peptide P-6 (DAYRCCPGC) was designed as the computing peptide (Fig. 4a), which contains two parts: the negatively charged group with Chy cleavage site (DAY) for neutralizing the peptide net charge, the positively charged group (R) and the AuNPs/Zn^{2+} binding group (CCPGC). In the initial state ("0/0"), without any input, P-6 can bind to AuNPs, but its zwitterionic property cannot make AuNPs aggregate to generate the corresponding output "1". When Chy was introduced in the state of "1/0", the cleavage of P-6 divided the negatively charged DAY from positively charged RCCPGC, and the latter induced AuNPs aggregation and thus an output "0" was displayed. Once Zn^{2+} was introduced in a state of "0/1" or "1/1", Zn^{2+} occupied the binding group of the peptide, and no AICC appeared, yielding a true output of red solution (output = 1, Fig. 4b, c). These results agreed with the IMPLICATION gate that we could achieve a false output only by introducing Chy. Similarly, a NAND gate could also be constructed by using a specifically designed computing peptide P-7 (DDDCCPGCYRACC, a NSP; Fig. S5f), which consists of the negatively charged Zn^{2+}/AuNP dual-binding sequence of DDDCCPGC, the positively charged AuNP binding group of RACC, and the Chy cleavage site Y in the middle. The overall net charge of the NAND gate peptide P-7 was -2, incapable of inducing AICC of AuNPs (output = 1) without inputs (0/0). Although the sole input of Chy (1/0) splits the peptide probe, both the resulting two segments could adsorb on AuNPs via their binding groups and retained the negative surface charge and well dispersion of AuNPs (output = 1). In the presence of Zn^{2+} (0/1), P-7 bound with Zn^{2+} and neutralized its charge. Its anchoring on AuNPs showed negligible effect on AuNPs solution (output = 1). In the input state of "1/1", Chy cleaved P-7 to DDDCCPGCY and RACC, and the Zn^{2+} bound with DDDCCPGCY to make DDDCCPGCY-Zn^{2+} complex, leaving only the positively charged RACC to bind with AuNPs and inducing aggregation to produce a false signal (A_{520}/A_{610} = 1.23, output = 0; Fig. S5e), while the other input states generated a true output of red solution with a ratio value for A_{520}/A_{610} exceeding 2 (Fig. S5e, f).

The combinational logic gate and the multisensing application

Since the basic binary logic gates were successfully obtained, it is reasonable to speculate that some integrated gates could also be executed in this system. With multiple inputs, logic gates can process a great deal of information, which is required for complex, multilevel integrated circuits[31]. For this purpose, EDTA was introduced as another logic input to compete with the CCPGC motif to interact with Zn^{2+}. Combining the computing peptide P-4 (ARYCCPGC), an INHIBIT logic gate was created, as shown in Fig. 5c. Here, EDTA competition would prevent Zn^{2+} from occupying the binding site of CCPGC, leaving P-4 to freely aggregate AuNPs. As expected, the four input states ("0/0", "1/0", "0/1", "1/1") produced relevant colorimetric signals of blue, red, blue and blue, corresponding to output "0", "1", "0" and "0" (Fig. 5b, c), respectively. The absorption spectrum shown in Fig. 4a also indicated that only the input state "1/0" demonstrated a single peak in 520 nm, meeting the demand of an INHIBIT gate (Fig. 5c). Furthermore, we further developed a combinational logic gate using Chy, Zn^{2+} and EDTA as three logic inputs and the peptide P-4 as the computing center. There were eight input states and eight corresponding output signals in this novel combinational logic gate. From the perspective of a logic circuit, in the input states of "1/0/0", "1/1/0", "1/0/1" and "1/1/1" with Chy as the input, the cleavage of P-4 separates the positively charged group ARY from AuNPs/Zn^{2+} dual-binding group CCPGC, thus leading to no AICC occurred with a true output of "1". With Zn^{2+} inputted in the state of "0/1/0", the binding group chelated

View Article Online
DOI: 10.1039/C6NR01072E

Zn^{2+} to yield an ARYCCPGC-Zn^{2+} complex and a red solution of output "1" resulted. All the other input states ("0/0/0", "0/0/1" and "0/1/1") leave P-4 to induce AICC of AuNPs, displaying a false output "0" (Fig. 5f). Further, according to the experimental phenomenon, a three-input INHIBIT-OR combinational gate was created, where Zn^{2+} and EDTA constituted the inputs of an INHIBIT gate and cascaded Chy into an OR gate.

Taking advantage of the chymostatin (Chym), a strong inhibitor of chymotrypsin and chymotrypsin-like serine proteinases[33], another three-input INHIBIT-OR combinational gate was also developed based on Chy/Zn^{2+}/Chym tri-inputs. As shown in Fig. S6, selecting P-4 as the computing peptide also, Chym combined with Chy to be an INHIBIT logic gate and then cascaded Zn^{2+} to be an OR gate, generating a Chy/Zn^{2+}/Chym three-input INHIBIT-OR combinational gate. In addition, besides the role as the computing center of INHIBIT-OR logic gates, the multi-functional peptide P-4 can also serve as multi-tasking biosensing probe that allows both Chy and Zn^{2+} to be detected, respectively. As shown in Fig. 6, Chy concentration was facilely probed by P-4/AuNP system with high sensitivity, even in the case that Chy and Zn^{2+} are coexisting, Chy activity can be detected without interference via the usage of EDTA as Zn^{2+} masking reagent, following to our Chy/Zn^{2+}/EDTA INHIBIT-OR combinational gate setting. The proposed sensor for Chy assay showed low limit of detection (LOD = 0.13 μg/L, S/N= 3) and excellent selectivity for Chy, which is significant for evaluating Chy levels of pancreatic disease and invasion by some types of cancer[30]. Moreover, the feasibility of this colorimetric sensor for assaying Zn^{2+} has been demonstrated in Zn^{2+} samples or Zn^{2+}/Chy coexisting samples using Chym for masking Chy according to the Chy/Zn^{2+}/Chym INHIBIT-OR gate setting (Fig. S7). The satisfactory analytical performance was achieved with a wide linear range from 0.05 μM – 1.2 μM, a low LOD at 17 nM (S/N= 3), and good selectivity. These results implied the potential application of complex logic system in multiplexing intelligent detection. Furthermore, these peptide-based logic sensing for Chy and Zn^{2+} also demonstrated some superiorities of time-saving, economy, simplicity, and convenience (Table S2, S3).

Conclusion

In summary, inspired by the natural recognition functions of peptide motifs in biological system and taking advantage of peptide- regulating nanoparticles assembly, we firstly built up a biomimetic and versatile peptide-based logic system based on metal ion/protease-responsive peptide-mediated AICC of AuNPs. Based on this system, peptides were defined as the computing center and AuNPs as the signal indicator, and then peptide logic operations were carried out in a homogenous and colorimetric manner. By rational design of peptide sequences with suitable regulation groups, we created basic logic gates for peptide computing, such as AND, OR, INHIBIT, IMPLICATION and NAND gates. In addition, a three-input combinational INHIBIT-OR logic gate was also successfully achieved and could be further applied as a preliminary multi-tasking sensor, indicating the potential for complex peptide computing and its application in multiplexing bio-sensing. This peptide-based logic system has several advantages, including visible and rapid read-out without modification of nanoparticles, designability of the computing elements (peptides) and the diversity and integratability of logic gates. Moreover, this research clearly shows that integrating the switchable chemical properties of peptides and the peptide-nanomaterial interaction presents a promising and powerful platform for simplifying the fabrication of peptide-based logic system. By analogy, it can be easily expand to build other metal ion/enzyme dual-input biologic systems by introducing analogous metal ion-chelating peptides or protease peptide substrates as relevant recognition units. Undoubtedly, the proposed logic system opens a practical avenue for peptide computing, especially the designability and flexibility of a peptide sequence with 20 amino acids, which would promote the realization of more complex functional logic devices, such as peptide manipulation and control tasks, peptide-related multiplex logic sensors and even peptide-targeted intellegent diagnosis.

Experimental Section

Reagents and Materials

AuNPs (gold nanoparticles, 13 nm, 11.2 nM) were prepared according to the classic method of heating a citrate reduction solution of $HAuCl_4$ [32]. All the peptides (in Table S1) were synthesized and purified by GL Biochem. Ltd. (Shanghai, China) and a Chinese peptide company (Hangzhou, China). In addition, all peptides were dissolved by 5 mM Tris-(2-carboxyethyl)-phosphine hydrochloride (TCEP) to 1 mM, then repacked and diluted to the needed concentration with ultrapure water and restored at -20 ^{o}C in refrigerator before use. Chymotrypsin (Chy), Chymostatin (Chym), and ethylene diamine tetraacetic acid (EDTA) were purchased from Shanghai Sangon Biological Engineering Technology & Services Co., Ltd (Shanghai, China). TCEP was purchased from Sigma (St. Louis, MO). All chemical reagents were of analytical grade and used without further purification. Ultrapure water (18.25 MΩ • cm) was obtained from a Millipore filtration system and used throughout. The inorganic salts and other organic chemicals employed here were of highest quality of analytical grade. UV-Vis absorption spectra were obtained on a Beckman DU-800 spectrophotometer. Transmission electron microscope (TEM) images were acquired on a JEOL JEM-2100F.

The operation of all logic gates

Taking the AND gate as an example, four Eppendorf tubes containing 50 μL 2×buffer (100 mM H_3BO_3- $Na_2B_4O_7.10H_2O$, 50 mM $NaClO_4$, 100 μM TCEP, pH 7.4) were prepared, corresponding to the four input states of the AND gate ("0/0","1/0", "0/1", "1/1"), and a certain volume of input 1 (1 mg/L Chy) was injected to the tubes of state "1/0" and "1/1",

View Article Online
DOI: 10.1039/C6NR01072E

and an equal volume of water was added to the tubes of input states "0/0" and "0/1". After that, four samples were incubated at 37 ℃ for enzymatic reaction for 30 min. Then, input 2 (2 μM Zn^{2+}) was added to states "0/1" and "1/1", and water was added to all states to reach a total of 100 μL. After homogeneous mixing, 100 μL AuNPs was injected to each tube. Then, 100 μL mixed solution was taken to collect the absorption spectra on Beckman DU-800 spectrophotometer, using the Wavelength Scan II mode scanning from 400 nm to 800 nm at a speed of 1200 nm/min. For the colorimetric analysis, the same samples were prepared to take photographs under the digital camera (Canon EOS70D). Also, the same operations were used for the OR, IMPLICATION and NAND gates unless otherwise stated. For INHIBIT and INHIBIT- OR gate, EDTA or Chym was assigned as input 3, and the operation was the same as other logic gate. The optimally ultimate concentration of peptides from P-1 to P-9 was 5 μM, 4 μM, 1.2 μM, 1.2 μM, 1.2 μM, 2.4 μM, 2 μM, 5 μM and 5 μM, respectively.

Acknowledgements

This work was financially supported by the National Natural Science Foundation of China (Grant Nos. 21222507, 21575038, 21235002, and 21175036), the Foundation for Innovative Research Groups of NSFC (Grant No. 21521063), and the Natural Science Foundation of Hunan Province (Grant No. 2015JJ1005).

Notes and references

1 (a) C. P. Collier, E. W. Wong, M. Belohradsky, F. M. Raymo, J. F. Stoddart, P. J. Kuekes, R. S. Williams and J. R. Heath, *Science*, 1999, **285**, 391. (b) A. P. de Silva and S. Uchiyama, *Nat. Nanotechnol.*, 2007, **2**, 399.
2 T. Miyamoto, S. Razavi, R. DeRose and T. Inoue, *ACS Synth. Biol.*, 2012, **2**, 72.
3 (a) M. Elstner, K. Weisshart, K. Mullen and A. Schiller, *J. Am. Chem. Soc.*, 2012, **134**, 8098. (b) E. Katz, J. Wang, M. Privman, J. Halamek, *Anal. Chem.*, 2012, **84**, 5463. (c) D. Margulies and A. D. Hamilton, *J. Am. Chem. Soc.*, 2009, **131**, 9142.
4 (a) J. Li, X. Jia, D. Li, J. Ren, Y. Han, Y. Xia and E. Wang, *Nanoscale*, 2013, **5**, 6131. (b)L. Qian and E. Winfree, *Science*, 2011, **332**, 1196. (c) L. Zhang, Y. Zhang, R. Liang, and J. Qiu, *J. Phys. Chem. C*, 2013, **117**, 12352. (d) W. Gao, L. Zhang, Y. Zhang, R. Liang, and J. Qiu, *J. Phys. Chem. C*, 2014, **118**, 14410.
(e) W. Gao, L. Zhang, R. Liang, J. Qiu, *Chem. Eur. J.*, 2015, **21**, 15272.
5 (a) G. Strack, M. Ornatska, M. Pita, and E. Katz, *J. Am. Chem. Soc.*, 2008, **130**, 4234. (b) R. Baron, O. Lioubashevski, E. Katz, T. Niazov, I. Willner, *J. Phys. Chem. A*, 2006, **110**, 8548. (c) E. Katz, and V. Privman, *Chem. Soc. Rev.*, 2010, **39**, 1835.
6 (a) C. M. Tan, H. Song, J. Niemi and L. C. You, *Mol. Biosyst.*, 2007, **3**, 343. (b) S. Ausländer, D. Ausländer, M. Müller, M. Wieland and M. Fussenegger, *Nature*, 2012, **487**, 123.
7 (a) R. Baron, A. Onopriyenko, E. Katz, O. Lioubashevski, I. Willner, S. Wang, H. Tian, *Chem. Commun.,* **20**, 2006, 2147. (b) Z. G. Wang, J. Elbaz, F. Remacle, R. D. Levine and I. Willner, *Proc. Natl. Acad. Sci. USA.,* 2010, **107**, 21996.
8 (a) L. M. Adelman, Science 1994, **266**, 1021. (b) R. J. Lipton, *Science*, 1995, **268**, 542. (c) Q. Ouyang, P. D. Kaplan, S. Liu, A. Libchaber, *Science*, 1997, **278**, 446.
9 M. N. Stojanovic, and D. Stefanovic, *Nat. Biotechnol.*, 2003, **21**, 1069. (b) J. Macdonald, Y. Li, M. Sutovic, H. Lederman, K. Pendri, W. Lu, B. Andrews, D. Stefanovic, and M. N. Stojanovic, *Nano Lett.*, 2006, **6**, 2598. (c) R. Pei, E. Matamoros, D. Stefanovic, and M. N. Stojanovic, *Nat. Nanotechnol.*, 2010, **5**, 773.
10 B. Gil, M. Kahan-Hanum, N. Skirtenko, R. Adar and E. Shapiro, *Nano Lett.*, 2011, **11**, 2989.
11 (a) G. Ashkenasy and M. R. Ghadiri, *J. Am. Chem. Soc.*, 2004, **126**, 11140. (b) M. Samiappan, Z. Dadon and G. Ashkenasy, *Chem. Commun.*, 2011, **47**, 710. (c) G. Ashkenasy, Z. Dadon, S. Alesebi, N. Wagner and N. Ashkenasy, *Israel Journal of Chemistry*, 2011, **51**, 106.
12 H. Hug and R. Schuler, *Bioinformatics*, 2001, **4**, 364.
13 Y. J. Lee, J. H. Lee, H. J. Cho, H. K. Kim, T. R. Yoon, *Biomaterials*, 2013, **34**, 5059.
14 M. Thoendel, J. S. Kavanaugh, C. E. Flack and A. R. Horswill, *Chem. Rev.*, 2011, **111**, 117.
15 K. A. Brogden, *Nature Reviews Microbiology*, 2005, **3**, 238.
16 (a) P. Laakkonen, K. Porkka, J. A. Hoffman and E. Ruoslahti, *Nat. Med.* 2002, **8**, 751. (b) P. Laakkonen, M. E. Akerman, H. Biliran, M. Yang, F. Ferrer, T. Karpanen, R. M. Hoffman and E. Ruoslahti, *Proc. Natl. Acad. Sci. U.S.A.*, 2004, **101**, 9381.
17 S. Lee , J. Xie and X. Chen, *Chem. Rev.*, 2010, **110**, 3087.
18 B. P. Gray and K. C. Brown, *Chem. Rev.*, 2014, **114**, 1020.
19 A. Hudmon and H. Schulman, *Annual Review of Biochemistry*, 2002, **71**, 473.
20 J. B. Denault and G. S Salvesen, *Chem. Rev.*, 2002, **102**, 4489.
21 C. Chen and N. L. Rosi, *Angew. Chem., Int. Ed.,* 2010, **49**, 1924.
22 R. R. Bhattacharjee, A. K. Das, D. Haldar, S. Si, A. Banerjee and T. K. Mandal, J. Nanosci. *Nanotechnol.*, 2005, **5**, 1141.
23 (a) A. Laromaine, L. Koh, M. Murugesan, R. V. Ulijn, and M. M. Stevens, *J. Am. Chem. Soc.*, 2007, **129**, 4156. (b) C. Guarise, L. Pasquato, V. De Filippis and P. Scrimin, *Proc. Natl. Acad. Sci. U.S.A.,* 2006, **103**, 3978.
24 W. Li, Z. Nie, K. He, X. Xu, Y. Li, Y. Huang and S. Yao, *Chem. Commun.*, 2011, **47**, 4412.
25 (a) L. Zhang, C. Xu, G. Song and B. Li, *RSC Adv.*, 2015, **5**, 27003. (b) R. Le´vy, N. T. K. Thanh, R. Christopher Doty, I. Hussain, R. J. Nichols, D. J. Schiffrin, M. Brust and D. G. Fernig, *J. Am. Chem. Soc.* 2004, **126**, 10076.
26 J. Oishi, Y. Asami, T. Mori, J.H. Kang, M. Tanabe, T. Niidome and Y. Katayama, *ChemBioChem*, 2007, **8**, 875.
27 (a) D. Liu, Z. Wang, A. Jin, X. Huang, X. Sun, F. Wang, Q. Yan, S. Ge, N. Xia, G. Niu, G. Liu, A. R. H. Walker and X. Chen, *Angew. Chem., Int. Ed.*, 2013, **125**, 14315. (b) D. Liu, W. Qu, W. Chen, W. Zhang, Z. Wang and X. Jiang, *Anal. Chem.*, 2010, **82**, 9606.
28 L. Zhang, Z. Wang, R. Liang, and J. Qiu, *Langmuir*, 2013, **29**, 8929.
29 A. Pomorski, J. Otlewski and A. Krezel, *ChemBioChem*, 2010, **11**, 1214.
30 A. Kumar and P. Venkatesu, *Chem. Rev.*, 2012, **112**, 4283.
31 W. Li, Y. Yang, H. Yan, and Y. Liu, *Nano Lett.*, 2013, **13**, 2980.
32 R. Jin, G. Wu, Z. Li, C. A. Mirkin and G. C. Schatz, *J. Am. Chem. Soc.*, 2003, **125**, 1643.
33 D. Paliwal, S.K. Panda, N. Kapur, S.P. Varma, H. Durgapal, *J. Gen. Virol*., 2014, **95**, 1689.

View Article Online
DOI: 10.1039/C6NR01072E

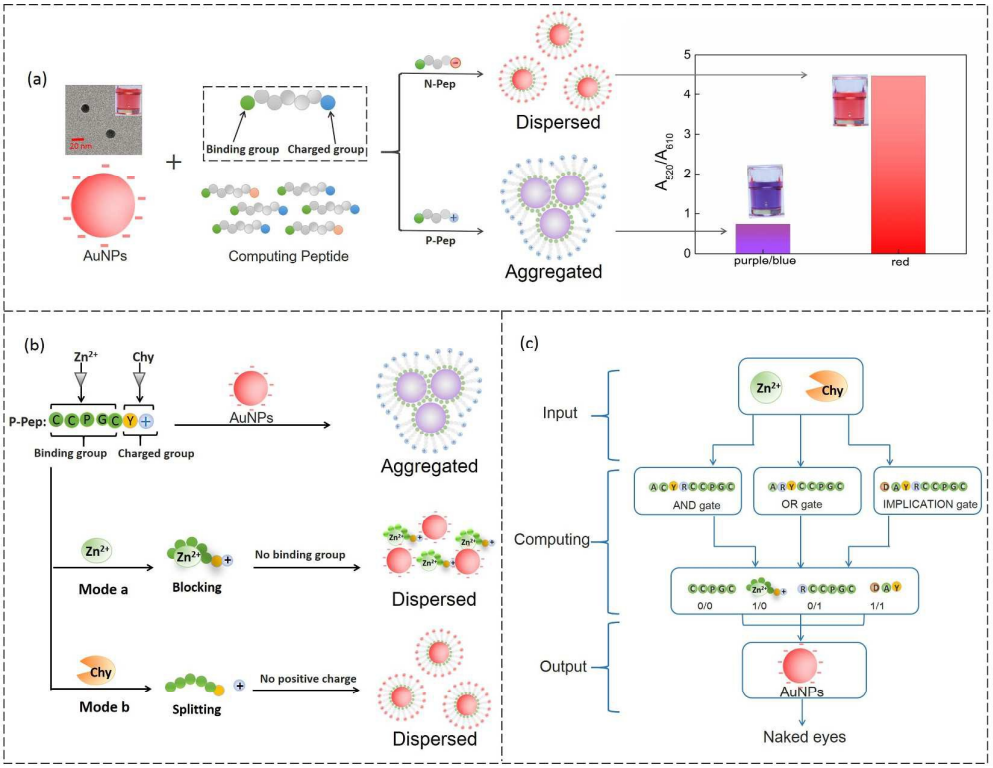

Scheme 1. The principle of the peptide logic gate: the description of peptide-mediated AICC of AuNPs (a); the response of the PSP-mediated AICC of AuNPs system to Zn^{2+} and Chy (b); the constitution of the peptide logic system (c).

View Article Online
DOI: 10.1039/C6NR01072E

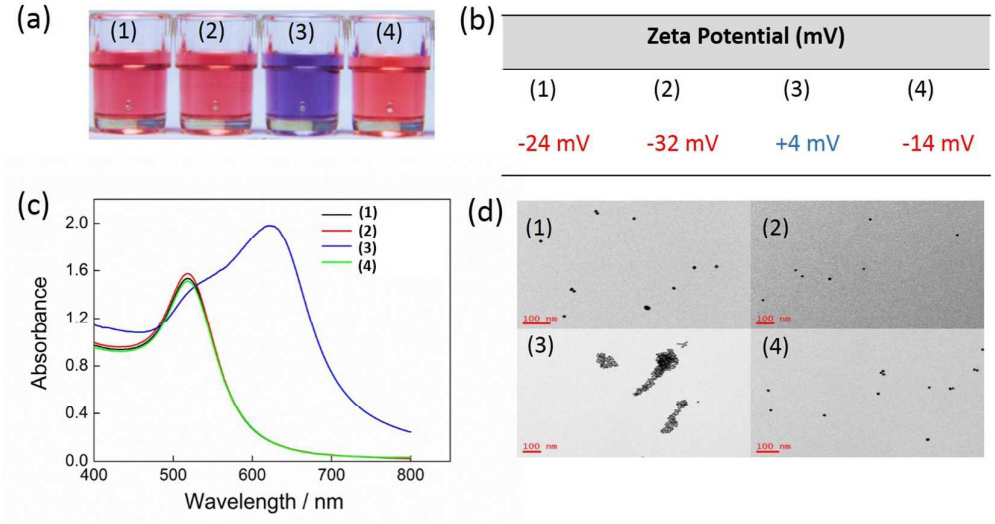

Fig. 1 The characteristic of AuNPs before or after affected by different peptides: the colour graph (a), the Zeta potential (b), the absorption spectra (c), and the transmission electron microscope (TEM) of AuNPs corresponding to no peptide addition (1), P-8 (2 μM DDDYCCPGC, 2), P-1 (2 μM CAAR, 3) and P-9 (2 μM CCPGC, 4), respectively.

View Article Online
DOI: 10.1039/C6NR01072E

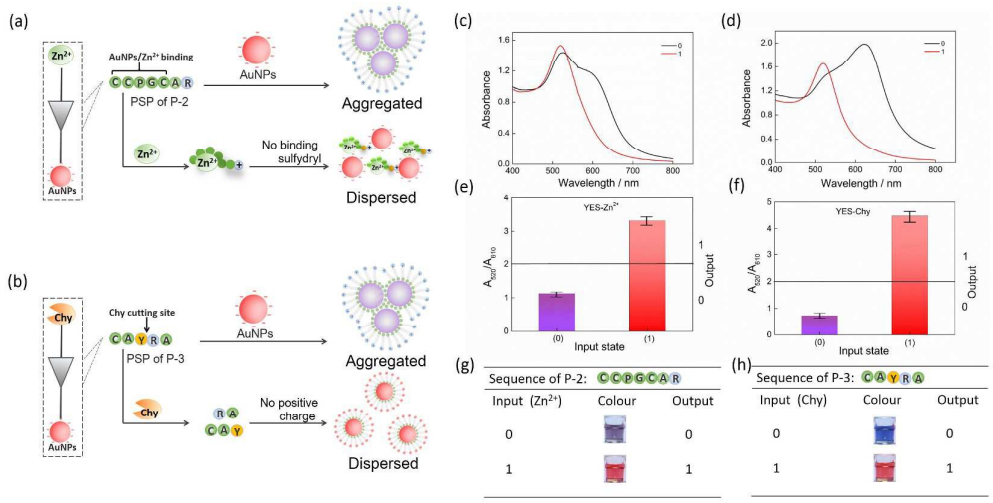

Fig. 2 The peptide-regulated AICC of AuNPs triggered by Zn^{2+} or Chy, which represents the YES-Zn^{2+} logic gate (a) and YES-Chy logic gate (b), respectively. The absorption spectra of the YES-Zn^{2+} logic gate (c) and the YES-Chy logic gate (d). The ratio of A_{520}/A_{610} of solutions corresponding to the YES-Zn^{2+} gate (e) and YES-Chy gate (f). The truth table and the corresponding colour of each output of the YES-Zn^{2+} gate (f) and YES-Chy gate (h).

View Article Online
DOI: 10.1039/C6NR01072E

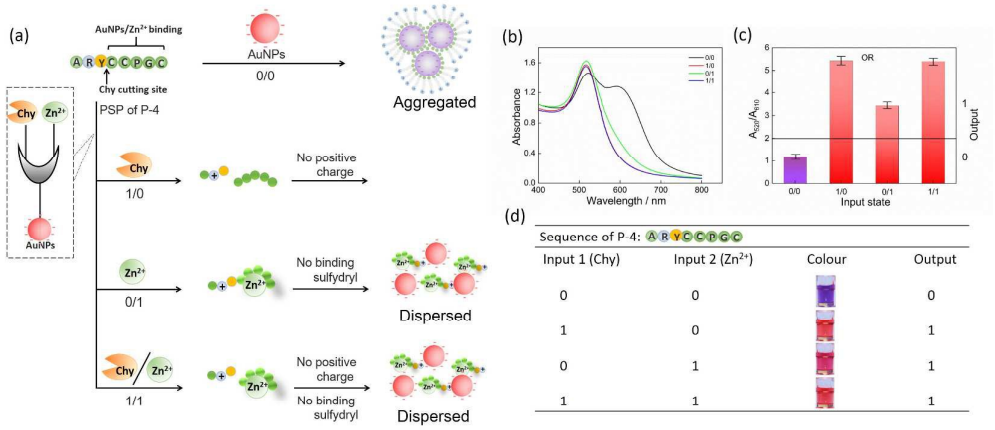

Input 1 (Chy)	Input 2 (Zn^{2+})	Colour	Output
0	0		0
1	0		1
0	1		1
1	1		1

Fig. 3 The representation of the binary OR logic gate based on the peptide-mediated AICC of AuNPs (a). The absorption spectra (b), the absorption ratios (A_{520}/A_{610}) (c), the truth table and the corresponding colour (d) of each output of the OR logic gate.

View Article Online
DOI: 10.1039/C6NR01072E

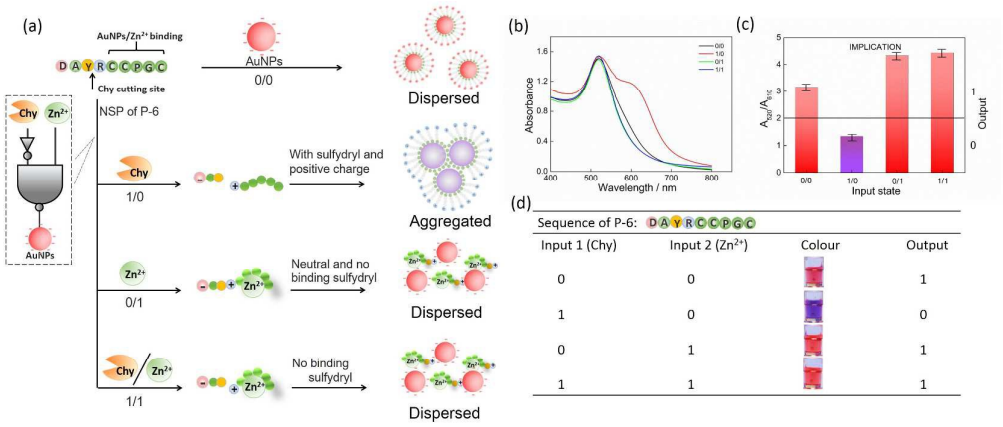

Input 1 (Chy)	Input 2 (Zn^{2+})	Colour	Output
0	0		1
1	0		0
0	1		1
1	1		1

Fig. 4 The representation of the binary IMPLICATION logic gate based on the peptide-mediated aggregation of AuNPs (a). The absorption spectra (b), the absorption ratios (A_{520}/A_{610}) (c), the truth table and the corresponding colour (d) of each output of the IMPLICATION logic gate.

View Article Online
DOI: 10.1039/C6NR01072E

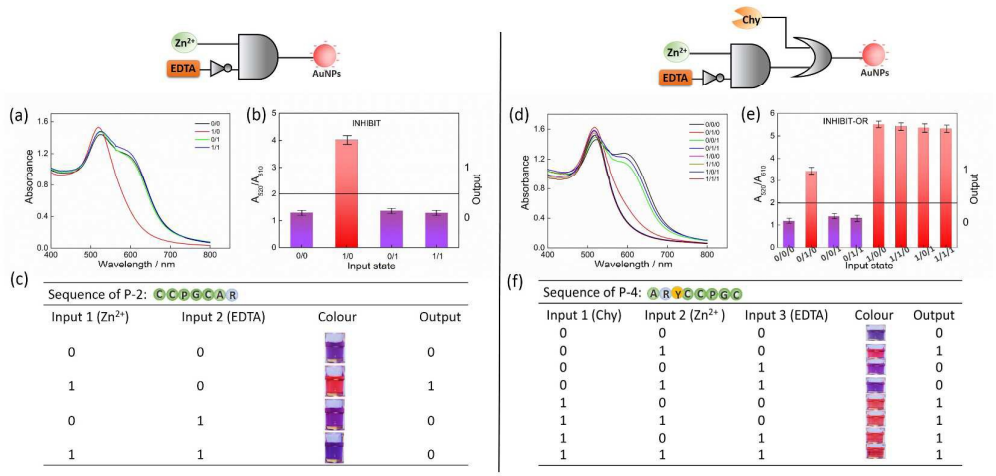

Fig. 5 The binary INHIBIT logic gate and the INHIBIT-OR combinational logic gate based on the peptide-mediated aggregation of AuNPs. The absorption spectra (a), the absorption ratios (A_{520}/A_{610}) (b), and the truth table of the INHIBIT logic gate (c). The absorption spectra (d), the absorption ratios (A_{520}/A_{610}) of the eight input states (e) and the truth table of the INHIBIT-OR logic gate (f).

View Article Online
DOI: 10.1039/C6NR01072E

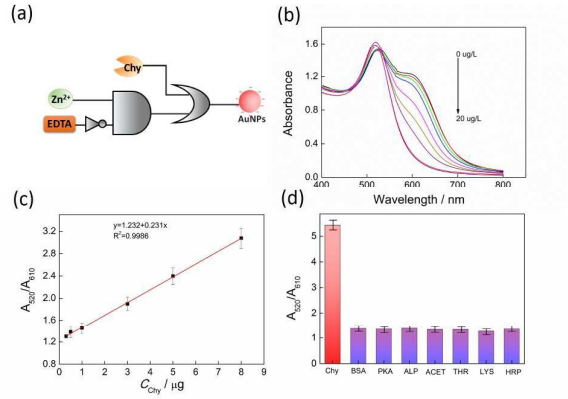

Fig. 6 The application of the INHIBIT-OR logic gate for Chy detection. The symbol of INHIBIT-OR logic gate (a). The absorption spectra of AuNPs with P-4 (1.2 μM) and Chy (0 μg–20 μg) (b). The linear relationship between the absorption ratio (A_{520}/A_{610}) and the concentrations of Chy (0.2 μg – 8 μg) (c). The absorption ratio (A_{520}/A_{610}) of AuNPs upon P-4 interacting with different enzymes (20 μg/L) for the selectivity investigation (d).